Transcriptomic landscape of skin lesions in cutaneous leishmaniasis reveals a strong CD8+ T cell immunosenescence signature linked to immunopathology

Carlos Henrique Fantecelle[1]; Luciana Polaco Covre[1,7]; Renan Garcia de Moura[1]; Herbert Leonel de Matos Guedes[2,3]; Camila Farias Amorim[4]; Phillip Scott[4]; David Mosser[5]; Aloisio Falqueto[6]; Arne N. Akbar[7] and Daniel Claudio Oliveira Gomes[1,8]

[1]Núcleo de Doenças Infecciosas, Universidade Federal do Espírito Santo, Brazil. [2]Instituto de Microbiologia Professor Paulo de Goes, Universidade Federal do Rio de Janeiro, Brazil. [3]Instituto Oswaldo Cruz, Fundação Oswaldo Cruz, Brazil. [4]Department of Pathobiology, School of Veterinary Medicine, University of Pennsylvania, USA.[5]Department of Cell Biology and Molecular Genetics, University of Maryland, College Park, Maryland, USA. [6]Departamento de Medicina Social, Universidade Federal do Espírito Santo, Brazil. [7]Division of Medicine, University College London, UK. [8]Núcleo de Biotecnologia, Universidade Federal do Espírito Santo, Brazil.

Key Words: Cutaneous leishmaniasis, senescence-associated secretory phenotype (SASP), immunopathogenesis, immunosenescence, *Leishmania braziliensis*

Corresponding author: E-mail address: dgomes@ndi.ufes.br

Núcleo de Doenças Infecciosas/Núcleo de Biotecnologia, Universidade Federal do Espírito Santo – UFES. Av. Marechal Campos, 1468 - Maruípe, Vitória – Brazil. Cep 29043-900

Tel: +55 27 33357210

Short title: Senescence in cutaneous leishmaniasis

Abbreviations: CL, cutaneous leishmaniasis; DEG, differentially expressed gene; EM, effector memory T cells; EMRA, effector memory T cells that re-expressing CD45RA; GEO, NCBI's Gene Expression Omnibus; GO, Gene Ontology; HC, healthy controls group; LCL, localized cutaneous leishmaniasis group; MCL, mucocutaneous leishmaniasis; NKR, NK cell receptors; NKRL, NK cell receptor ligand; PCA, principal component analysis; SASP, senescence-associated secretory phenotype; Tsen, senescent T cells.

Summary:

The severity of lesions that develop in patients infected by *Leishmania braziliensis* is mainly associated with a highly cytotoxic and inflammatory cutaneous environment. Recently, we demonstrated that senescent T and NK cells play a role in the establishment and maintenance of this tissue inflammation. Here, we extended those findings using transcriptomic analyses that demonstrate a strong co-induction of senescence and pro-inflammatory gene signatures in cutaneous leishmaniasis (CL) lesions. The senescence-associated signature was characterized by marked expression of key genes such as ATM, Sestrin 2, p16, p21, p38. The cell type identification from deconvolution of bulk sequencing data showed that the senescence signature was linked with CD8$^+$ effector memory and T$_{EMRA}$ subsets and also senescent NK cells. A key observation was that the senescence markers in the skin lesions are age-independent of patients and were correlated with lesion size. Moreover, a striking expression of the senescence-associated secretory phenotype (SASP), proinflammatory cytokine and chemokines genes were found within lesions that was most strongly associated with the senescent CD8 T$_{EMRA}$ subset. Collectively, our results confirm that there is a senescence transcriptomic signature in CL lesions and supports the hypothesis that lesional senescent cells have a major role in mediating immunopathology of the disease.

Introduction

Leishmaniasis is a group of severe neglected tropical diseases, caused by *Leishmania* parasites and is prevalent in over 98 countries in the world (1). *Leishmania braziliensis* is the main causal agent of both cutaneous (CL) and mucocutaneous (MCL) leishmaniasis in Brazil, where mucosa and skin destructive lesions progressively develop (2).

The immune response against *Leishmania* is a complex process involving both innate and adaptive immunity, where T cells have a key role in promoting both protection and/or pathology (3,4). With regard to the pathology that occurs, substantial evidence has demonstrated the role of the overwhelming inflammatory processes, as well as non-specific cytotoxic response in the disease (4–10). This was observed in skin lesions of patients with MCL and CL that demonstrated the enrichment of cytotoxic and pro-inflammatory cells with a conspicuous capacity to mediate tissue destruction (5,6,9). Moreover, both cytotoxicity and inflammatory-related genes are overexpressed in the lesional environment of CL patients, that positively correlated with extensive necrosis and lesion size (11–16).

Immunosenescence is a term that refers to the gradual change of the immune system resulting from ageing, persistent inflammatory states and chronic antigenic stimulation (17,18). Some of these changes are obvious within in the T cell compartment. These cells acquire a senescent phenotype and defective responses that are linked with the loss of proliferative capacity and decreased TCR-related signalling and proliferation after activation (19,20).

Senescent T cells (Tsen) undergo widespread changes in morphology, cell metabolism and secretory phenotype (21). These cells are still metabolically active and secrete a wide array of pro-inflammatory cytokines, chemokines, matrix metalloproteases and growth factors, that is collectively known as the senescence-associated secretory phenotype (SASP) that has considerable consequences for inducing the tissue inflammatory microenvironment (22,23). Moreover, both CD4$^+$ and CD8$^+$ Tsen cells express high levels of intracellular granules containing the cytotoxic proteins

perforin and granzyme B, as well as express NK cell receptors (NKRs) (24–26). Therefore, the increased inflammatory potential of T cells in CL may contribute to the pathology of this disease.

Recently we have demonstrated that both CD4^{+} and CD8^{+} circulating Tsen cells with high inflammatory profile accumulate during infection with *L. braziliensis*. Moreover, they showed an increased propensity to migrate to the skin, where their potent inflammatory activity and accumulation were linked to the severity of skin lesions observed in cutaneous leishmaniasis patients (27,28).

We have now analysed previously published RNA-Seq datasets to evaluate the immunosenescence signature within lesional CL transcriptomes. Confirming previous observations, we found that lesions are transcriptionally distinct from healthy skin, exhibiting a strong co-induction in the transcript levels of senescence-associated genes and pro-inflammatory immune responses. Moreover, transcriptional signatures of immunosenescence genes and pathways not only were found overrepresented in lesions, but these lesional signatures were linked to the immunopathology of CL. Therefore, this study sheds insight into the skin lesional environment and reveals gene signatures associated with the physiopathology of the disease, which may be explored and extrapolated to understand inflammation and immune-mediated pathology in CL and several other related diseases.

Materials & methods

Transcriptomic analyses of skin lesions from publicly available datasets. Raw counts matrix from a previous study on the lesional gene expression in CL was obtained from NCBI's Gene Expression Omnibus (GEO) through accession code: GSE127831 (29). All analyses of RNA-Seq data were performed using R version 4.0.3 (30) in RStudio 1.4.1103 (31). This resulted in count data from 21 skin samples from patients infected with *L. braziliensis* before treatment and 7 uninfected endemic controls. Patients from this dataset consisted of 17 males and 4 females of age 38± 16,8 and lesions size ranging from 13–1237 mm^2. Genes that had less than 10 total counts in all samples were removed prior to subsequent analyses, resulting in a count table of 26,545 genes. DESeq2 (32)

that was used to identify differentially expressed genes, considering those with Benjamini-Hochberg p-adjusted value less than 0.05 as statistically significant. For visualization and clustering, count data was normalised, and variance stabilized through the vst function available in DESeq2 package. The Principal Component Analysis (PCA) was calculated using plotPCA function, also in the DESeq2 package. Gene Ontology (GO) overrepresentation was assessed using clusterProfiler package for Biological Processes in the GO database by using all DEGs and considering significant categories that had adjusted p-value < 0.05. The CellAge database (33) from Human Aging Genomic Resources (34) was adapted with added senescence-associated genes and was used to investigate the senescence signature in the dataset. The STRING database v11.0 (35) was used to determine human protein-protein interactions (minimum score of 700) within the senescence-associated DEGs through use of the RITAN package. Immune cell deconvolution was performed through ImmQuant software (36) using the DMAP database, with scores calculated relative to the mean of all samples. Spearman's correlation was calculated between variance stabilized gene expression values and cell population scores predicted by ImmQuant. A correlation matrix was generated with the cor function in R, and the p-values matrix was created using the cor_pmat function in ggcorrplot package. The results were then plotted as a heatmap. Several tools were used for visualizing the results of RNA-Seq analyses. Heatmaps were constructed with relative expression vst transformed values, centred across gene means, through the ComplexHeatmap package. Volcano plot was made with EnhancedVolcano package. The package ggraph was employed to construct the network plots. All other plots were generated with ggplot2.

Parasite burden determination. Parasite burden data was obtained from Amorim and cols, 2019 (29) that it quantified by qPCR in the same RNA preparations used for RNA-seq, as described by the authors. Briefly, a standard curve was prepared from total RNA extracted from 10^7 *L. braziliensis* promastigotes recovered from axenic culture using the RNeasy Plus Mini Kit (Qiagen), and cDNA was generated with the High Capacity RNA to cDNA kit (Applied Biosciences). qPCR was performed

6

using Power SYBR green master mix (Applied Biosciences) and primers targeting the *L. braziliensis* 18S ribosomal subunit (F: 5'-TACTGGGGCGTCAGAG-3' and R: 5'-GGGTGTCATCGTTTGC-3') and human GAPDH (housekeeping gene, F: 5'- GGTGTGAACCATGAGAAGTATGA-3' and R: 5'-GAGTCCTTCCACGATACCAAAG-3').

Immunofluorescence study subjects. Skin biopsies from 10 untreated patients with cutaneous leishmaniasis seen at the University Hospital (HUCAM) of Universidade Federal do Espírito Santo, Brazil, were investigated in this study. Patient group (LCL) consisted of 5 males and 3 females of age 37± 10.3 years and lesion sizes ranging from 7–2734 mm^2 with durations ranging from 45 to 120 days. Diagnosis of CL was made with clinical and laboratory criteria and all patients in this study were positive for the PCR/restriction fragment length polymorphism of *L. braziliensis* and reported no prior infections or treatments. The control group (HC) consisted of 6 healthy age (26,83 ± 5,64) and gender-matched individuals with no history of leishmaniasis. All participants (patients and healthy volunteers) tested for HIV, HBV and HCV infections, and presented no history of chemotherapy, radiotherapy or treatment with immunosuppressive medications within the last 6 months. All samples in the study were obtained before the COVID-19 outbreak. Patients provided written informed consent, and all study procedures observed the principles of the Declaration of Helsinki. This study was registered at HUCAM ethical committee reference number 735.274.

Skin Biopsies. Punch biopsies (8 mm in diameter) from the border of lesional skin from cutaneous leishmaniasis patients and from skin of healthy volunteers were obtained. Biopsy specimens were frozen in OCT compound (Sakura, Alphen aan den Riji, The Netherlands). Six-micrometre sections were longitudinally sectioned to expose all skin layers and placed in poly-L-lysine coated slides (Star Frost®). Tissues were then fixed in acetone and ethanol and stored in -80 ºC until use.

Immunofluorescence

Six micrometers cryosections were obtained from skin biopsies of healthy individuals and patients with cutaneous leishmaniasis and prepared on poly-L-lysine coated glass slides (StarFrost, Knittel, Germany). Sections were stained for KLRG1 (Abcam, ab170959, 1:400) and ATF2 (Abcam, ab242381, 1:100) for 18 h at 4°C, followed by incubation with the secondary antibody goat anti-rabbit IgG Alexa Fluor 568 (Thermo Fisher, A11036, 1:400) and mounting with Flouroshield Mounting Medium with DAPI (ABCAM, ab104139). Imaging consisted of obtaining five images of the dermis captured at 200x magnification using fluorescence microscopy (Leica DMi8, Wetzlar, Germany) or slide scanner (Axio Scan, Zeiss, Germany). All positively stained cells and nuclei within each image were manually counted using computer-assisted image analysis (National Institutes of Health Image Software ImageJ 1.52j; https://imagej.nih.gov/ij/). The data is shown as the average number of positive cells divided by the nuclei count x 100 to be expressed as percentage.

Statistical analysis

Analysis of ImmQuant results and gene correlation data was performed in R environment. For immunofluorescence data, analyses were performed in GraphPad Prism v8.0. Cell population scores were compared using unpaired Wilcoxon rank-sum test. Immunofluorescence data normality was assessed with the Shapiro-Wilk test, and groups were compared using Student's *t* test with Welch's correction or Wilcoxon rank-sum test. Correlations were assessed by Spearman's rank correlation for gene expression data, and Pearson's correlation for immunofluorescence data. Significance values were represented as follows: *: $p < 0.05$; **: $p < 0.01$; ***: $p < 0.001$; ****: $p < 0.0001$.

Code availability

A markdown report with all code used to produce the results in this study is provided as a supplementary file.

Results

Transcriptional signature of CL lesions reveals a senescent profile

First, we analysed if a senescence signature was present in biopsies collected from the border of lesions from patients infected with *Leishmania braziliensis* when compared to skin biopsies from uninfected controls using RNA-Seq data from a previous study (29). We defined differentially expressed genes (DEGs) as those with an adjusted p-value < 0.05 and found a total of 12,306 DEGs, in which 6,076 were overrepresented and 6,230 were underrepresented (S1 Table). The heatmap and hierarchical clustering of DEGs (Supplementary figure 1A), PCA (Supplementary figure 1B) and volcano plot (Supplementary figure 1C) of the total transcriptome data revealed distinct gene expression profiles between healthy skin and lesions from infected patients, supporting previous observations (13,29,37). Gene Ontology (GO) overrepresentation analysis of all DEGs also revealed GO terms that are closely linked with both protective and pathological mechanisms of CL, as well as terms associated with senescence, namely the GO terms "aging" and "replicative senescence" (Fig 1A).

Specific senescence-associated features have been mainly characterized in circulating T cells during cutaneous leishmaniasis (28). To investigate the possible cell types involved on the immune response within CL lesions, we performed a deconvolution analysis of bulk RNA-Seq data using ImmQuant (36). This analysis revealed distinct immune cell-type compositions between patients and healthy controls (Fig 1B). Notably, CD8 Effector memory T (CD8 T_{EM}) and Effector memory T cells that re-express CD45RA (CD8 T_{EMRA}), NK cells and monocytes were significantly enriched in CL lesions (Fig 1C).

Senescence-associated genes are found in CL lesions

We previously reported the skin lesion accumulation of senescent cells and its role in mediating pathology of lesions (28). To confirm the presence of a lesional senescence signature we next

analysed a curated selection of genes from CellAge senescence database along with other known key genes associated with senescence. Using foldchange cut-offs of 2 and -2, we found 107 differentially expressed genes in CL lesions, where 70 were overrepresented and 37 were underrepresented that were classified within oncogene-, stress-induced and replicative senescence categories (Supplementary figure 2A, supplementary table 2). Interaction analysis using senescence DEGs revealed interactions among 48 overrepresented and 8 underrepresented genes (S3 Table) that were mostly linked with the replicative senescence pathway (Supplementary figure 2B). Further analysis within key senescence-DEGs (38) found a wide upregulation of key genes associated with immunosenescence that included cyclin-dependent kinase inhibitors p21 (*CDKN1A*) and p16 (*CDKN2A*), DNA damage response protein *ATM*, p38 (*MAPK11*), Sestrin 2 (*SESN2*), *ATF5*, as well as key genes linked with cell differentiation such as EOMES and Tbet (*TBX21*) (Fig. 2A). Moreover, they did not correlate with the age of patients, suggesting that in the lesional environment the expression of senescence key genes is governed by non-age-related factors (Supplementary figure 3A). Interestingly, most of the senescence genes correlated positively with the parasitic load observed in lesions of patients (Fig 2B), opposed to what was found regarding healing time, where only p21 (CDKN1A) showed a positive correlation (Supplementary figure 3B). Next, to evaluate the link between the expression of senescence genes and lesional cell populations, we next performed Spearman correlations between the ImmQuant scores (34) and senescence DEGs. We found that the expression of senescence genes positively correlates with the predicted relative proportions of several immune cell types, including CD8 T and NK cell subsets and monocytes. However, the strongest correlations were found within senescent CD8 (EMRA) and senescent NK (CD56$^+$CD16$^+$) subsets (Fig 2C). Senescence genes also had a positive correlation with monocytes (Fig. 2C), to a lesser extent, that requires further analysis.

Overall, these data support our findings on the accumulation of senescent T and NK cells in the lesional environment and suggest that they may be maintained or expanded by the presence of antigens or parasites. Moreover, we cannot exclude the possibility that tissue non-lymphoid cells

(such as keratinocytes, fibroblasts and/or endothelial cells) also exhibited a senescence profile as gene signatures for these cells were not part of the deconvolution signature.

Transcriptional landscape of CL lesions shows a profile of SASP, inflammatory cytokine and chemokine genes

Overwhelming inflammation is one of the main signatures of CL skin pathogenesis. Given the results indicating a senescent profile in lesions, we next investigated if senescent cells may instigate tissue damage through a senescence-associated secretory phenotype (SASP). We performed a wide analysis of inflammatory cytokines, chemokines and their receptors that may induce skin pathology. Our analysis found 75 differentially expressed genes, of which 63 were increased by at least two-fold (S4 Table). Comparative analysis uncovered that among 68 SASP genes tested, 50 were DEGs and 25 were greatly increased, with fold changes ranging from 13-fold (*IL1A*) to 535-fold (*MMP1*) increases (Fig 3A and S4 table). The top 12 overrepresented SASP genes were associated with recruitment of inflammatory immune cells (CCL3, CCL8, CXCL1, CXCL11, CXCL13, CXCL8); metalloproteinases (MMP1, MMP10 and MMP3) and inflammatory cytokines (IL-6, IL-15 and IL-1β) (Fig 3B, C and supplementary figure 4). In addition, other non-SASP inflammatory cytokines, chemokines and their receptors such as IFN-γ (*IFNG*), TNF-α (*TNF*), IL-23 (*IL23A*), IL-15 receptor (*IL15RA*), CXCL10, CXCL9, CCL4 and CCR5 were overrepresented in CL lesions (Fig 3C and supplementary figures 5A and 5B), supporting previous findings (13,14,29,37,39). As expected, most of the DEGs positively correlated with the predicted relative proportions of analysed cell subsets (Fig 3C). Interestingly, this correlation was most conspicuous within NK $CD56^+CD16^+$, CD8 T_{EM} and CD8 T_{EMRA} subsets, where the latter demonstrated the strongest association with all SASP, cytokines, chemokines and cytokine/chemokine receptors DEGs analysed (Fig 3C). Most of these genes also correlated with monocyte population, suggesting their presence in the lesional environment with an overlapping inflammatory profile with senescent cells (Fig 3C).

The expression of senescence markers is enhanced in CL lesions and correlates with lesion size

Senescent leukocytes may be defined by several phenotypic markers, as well as a state of cell cycle arrest (40). We next performed in situ analysis by immunofluorescence for killer cell lectin-like receptor 1 (KLRG-1) that is a well-known senescence marker of T and NK cells (41). In addition, we also analyzed the human ATF phosphorylated protein, an important transcription factor of the senescence pathway, involved in oxidative stress response and cellular growth arrest of both immune and non-immune cells (42). Compared to healthy controls, patients had an intense cell infiltration in the lesional skin associated with greater proportions of leukocytes and non-immune senescent cells expressing both KLRG-1 and ATF (Fig 4A, B, C and E). Gene expression analysis of KLRG-1 and ATF genes also supports these findings, where an increase of seven-fold and five-fold over the HC group, respectively, was found (Fig 4D, F). Furthermore, we correlated the size of the skin lesions in patients with the extent of ATF or KLRG-1 cells infiltration. Interestingly, the accumulation of both senescent markers strongly correlates with lesion size observed in patients (Fig 4G, H), supporting previous findings about senescent cells accumulation in the skin as well as suggesting that these cells have a greater impact on the immunopathology in the skin of patients with CL (27,43).

Discussion

In this work we used transcriptome profiling analysis to evaluate if cell senescence is involved in the lesional signature and the pathology of cutaneous leishmaniasis. Thus, we now extend the knowledge of skin immunity in CL by identifying a key set of immunosenescence transcripts and pathways in the lesional environment during CL.

Infection of the skin by *L. braziliensis* promotes wide tissue remodelling and damage, with an intense leukocyte inflammatory infiltrate composed by immune cells (44). We have recently demonstrated that circulating senescent T cells (Tsen) with high inflammatory profile and increased propensity to migrate to the lesional skin accumulate during infection with *L. braziliensis* (28). Indeed,

the accumulation of lesional senescent CD8 T cells positively correlated with lesion size, suggesting the involvement of these T cells in mediating the pathology of this disease (27,28).

Senescent cells accumulate in many tissues during ageing, persistent antigenic stimulation and chronic infections, including cutaneous leishmaniasis (45,46). An interesting observation is that although they do not proliferate, these cells are still metabolically active and secrete a wide array of cytokines, chemokines and matrix metalloproteases, nominated as senescence-associated secretory phenotype (SASP). This pronounced proinflammatory secretome attract leucocytes, potentiates chronic inflammation and tissue damage, causing pathology in a similar way to those observed in cutaneous leishmaniasis (27,47).

Activation of senescence pathways causes the alteration of immune and non-immune cell secretory phenotypes (48,49). Our RNA-seq analysis confirms this, where most of the well-established senescence-associated genes were found overrepresented in the lesions, including the serine-protein kinase ATM, cell cycle regulator p16, p21 and p38 MAP kinase. We also observed an overrepresentation of other markers such as KLRG-1, EOMES and Tbet that are associated with cell activation processes. Although this may be a limitation of this work, these markers are well-established features to define immunosenescence when used in association with other markers, as demonstrated here (41,48,50).

In a deeper investigation of the host response, we used the ImmQuant software to infer the cell type composition of the bulk skin transcriptome (32). We identified a key set of both senescence pathways and SASP-related transcripts in CL lesions that positively correlated with predicted compositions of senescent cells and monocytes. These populations that includes monocytes/macrophages can share multiple phenotypic characteristics including the SASP secretome. Moreover, inflammation and senescence pathways and signs that share many components may corroborate to the increase of those genes in monocytes population, as found in our analysis (51,52). The local accumulation of cells with senescence features correlated positively with the lesion severity observed in patients. These observations support our previous results and

sustain the hypothesis that lesional senescent cells are key for mediating immunopathology of CL through an exacerbated inflammatory immune response. Still related to pathology, although our data has mostly emphasized a strong transcriptional signature of immune cells as indicated by ImmQuant software analysis, we do not rule out the participation of non-immune as well as non-senescent cell populations at this process, which offers the basis for further complementary studies. Overwhelming inflammation is one of the main signatures of CL skin pathogenesis, where lesional transcriptomic analysis reveals a strong signature of inflammasome activation and release of IL-1β, TNF-α and IFN-γ (5,39,53,54). Now we gather to these other cytokines, chemokines and growth factors, including a wide SASP secretome. Although non-senescent cells can contribute to numerous inflammatory SASP-related factors, most commonly reported SASP factors are expressed in response to replicative-, oncogene- and DNA damage-induced senescence that support the role of senescent cells to the lesional inflammation (55,56). In this scenario, SASP may contribute to induce senescence of adjacent cells in a paracrine manner by building a positive feedback loop, gradually exacerbating the inflammatory effects on tissues. In addition, several SASP components can also directly modulate the expression of stress ligands including those that bind to NK receptors by immune and non-immune cells (57,58). The interaction between these ligands and NK receptors such as NKG2D on T/Tsen with NKRL-expressing cells in the skin may leads to a cytotoxic killing mechanism with non-specific tissue damage that amplifies the overwhelming inflammation, contributing to the progressive growth of CL lesions (59,60).

In CL the development of the classical ulcer occurs concomitantly with the local inflammation (54,61). Although there are few parasites, their presence in the skin tissue is not correlated to the size of the lesions observed in patients. Recent data show that the lesional parasite load directly correlates with the transcriptional signature of inflammatory, cytotoxic mediators and accumulation of cytotoxic CD8^{+} T cells (61), and these are the main responsible for the tissue pathology (14,29). The accumulation of senescent and non-senescent cells in the cellular infiltrate as well as local inflammation may clarify the correlation observed between the parasites and senescence signature.

Moreover, the local accumulation of senescent cells may generate a destructive positive feedback loop with progressive and unspecific tissue damage and persistent inflammation, unable to eliminate parasites from the lesion but wieldy in promoting disease severity (61). Therefore, controlling SASP/senescence pathways and/or the accumulation of senescent cells may also have protective effects, dampening local tissue damage.

Overall, the present study extends the understanding of the local senescence signature that occurs in the context of *L. braziliensis* infection. Moreover, our analyses provide information on how senescent cells may corroborate the progressive pathology in the skin lesions. Controlling senescence or the positive inflammatory feedback in this process may be the most effective strategy for targeting an efficient anti-*Leishmania* immunity and laying the foundation for new therapies in leishmaniasis.

Disclosures

The authors state no conflict of interest.

Data availability statement

The data used in this study is available at NCBI's GEO through the accession: GSE127831. All code, as well as software and package versions, used in the study is provided as a supplementary file.

Author contributions

CHF analysed RNA-Seq the data. RGM and LPC carried out skin biopsies experiments and results analysis. CFA, PS and HLMG participated in analysis and discussion of the data and experiments. DCOG, LPC, AA, DM and CHF devised the study and discussed the data. AF selected the patients. DCOG, CHF, LPC, RG, AA, DM wrote the manuscript with the other co-authors' support. All authors contributed and approved the submitted version of the article.

References:

1. World Health Organization. OMS | Leishmaniasis. WHO [Internet]. 2015;375. Available from: http://www.who.int/mediacentre/factsheets/fs375/es/
2. Goto H, Lauletta Lindoso JA. Cutaneous and Mucocutaneous Leishmaniasis. Infectious Disease Clinics of North America. 2012;26(2):293–307.
3. Dantas ML, Oliveira JC de, Carvalho L, Passos ST, Queiroz A, Machado P, et al. Major Article CD8 + T cells in situ in different clinical forms of human cutaneous leishmaniasis. Revista da Sociedade Brasileira de Medicina Tropical. 2013;46(November):728–34.
4. Faria DR, Souza PEA, Durães F v., Carvalho EM, Gollob KJ, MacHado PR, et al. Recruitment of CD8+ T cells expressing granzyme A is associated with lesion progression in human cutaneous leishmaniasis. Parasite Immunology. 2009;31(8):432–9.
5. Novais FO, Carvalho AM, Clark ML, Carvalho LP, Beiting DP, Brodsky IE, et al. CD8+T cell cytotoxicity mediates pathology in the skin by inflammasome activation and IL-1?? production. PLoS Pathogens. 2017;13(2):1–21.
6. Faria DR, Gollob KJ, Barbosa J, Schriefer A, Machado PRL, Lessa H, et al. Decreased in situ expression of interleukin-10 receptor is correlated with the

exacerbated inflammatory and cytotoxic responses observed in mucosal leishmaniasis. Infection and Immunity. 2005;73(12):7853–9.

7. Carvalho AM, Novais FO, Paixão CS, de Oliveira CI, Machado PRL, Carvalho LP, et al. Glyburide, a NLRP3 Inhibitor, Decreases Inflammatory Response and Is a Candidate to Reduce Pathology in Leishmania braziliensis Infection. Journal of Investigative Dermatology. 2020;

8. Santos D, Campos TM, Saldanha M, Oliveira SC, Nascimento M, Zamboni DS, et al. IL-1β production by intermediate monocytes is associated with immunopathology in cutaneous leishmaniasis. Journal of Investigative Dermatology [Internet]. 2017;(2018). Available from: http://linkinghub.elsevier.com/retrieve/pii/S0022202X17332426

9. Schriefer A, Machado P, Jesus R de, Dutra WO, Gollob KJ, Carvalho EM. Up-Regulation of Th1-Type Responses in Mucosal Leishmaniasis Patients. 2002;70(12):6734–40.

10. Faria DR, Souza PEA, Durães F v, Carvalho EM, Gollob KJ, Machado PR, et al. Recruitment of CD8(+) T cells expressing granzyme A is associated with lesion progression in human cutaneous leishmaniasis. Parasite immunology [Internet]. 2009;31(8):432–9. Available from: http://www.pubmedcentral.nih.gov/articlerender.fcgi?artid=2764276&tool=pmce ntrez&rendertype=abstract

11. Novais FO, Carvalho LP, Passos S, Roos DS, Carvalho EM, Scott P, et al. Genomic Profiling of Human Leishmania braziliensis Lesions Identifies Transcriptional Modules Associated with Cutaneous Immunopathology. Journal of Investigative Dermatology. 2015;135(1):94–101.

12. Amorim CF, Novais FO, Nguyen BT, Misic AM, Carvalho LP, Carvalho EM, et al. Variable gene expression and parasite load predict treatment outcome in cutaneous leishmaniasis. Science Translational Medicine. 2019;11(519):1–10.

13. Christensen SM, Dillon LAL, Carvalho LP, Passos S, Novais FO, Hughitt VK, et al. Meta-transcriptome Profiling of the Human-Leishmania braziliensis Cutaneous Lesion. PLoS Neglected Tropical Diseases. 2016;10(9):1–17.

14. Farias Amorim C, Novais FO, Nguyen BT, Nascimento MT, Lago J, Lago AS, et al. Localized skin inflammation during cutaneous leishmaniasis drives a chronic, systemic ifn-γ signature. PLoS Neglected Tropical Diseases. 2021 Apr 1;15(4).

15. Campos TM, Novais FO, Saldanha M, Costa R, Lordelo M, Celestino D, et al. Granzyme B Produced by Natural Killer Cells Enhances Inflammatory Response and Contributes to the Immunopathology of Cutaneous Leishmaniasis. Journal of Infectious Diseases. 2020;221(6):973–82.

16. Santos CDS, Boaventura V, Ribeiro Cardoso C, Tavares N, Lordelo MJ, Noronha A, et al. CD8+ granzyme B+ -mediated tissue injury vs. CD4 + IFNγ+ -mediated parasite killing in human cutaneous leishmaniasis. Journal of Investigative Dermatology. 2013;133(6):1533–40.

17. Ginaldi L, Loreto MF, Corsi MP, Modesti M, Martinis M de. Immunosenescence and infectious diseases. Microbes and Infection. 2001;3(10):851–7.

18. Akbar AN, Henson SM. Are senescence and exhaustion intertwined or unrelated processes that compromise immunity? Nature reviews Immunology [Internet]. 2011;11(4):289–95. Available from: http://dx.doi.org/10.1038/nri2959

19. Lanna A, Gomes DCO, Muller-Durovic B, McDonnell T, Escors D, Gilroy DW, et al. A sestrin-dependent Erk-Jnk-p38 MAPK activation complex inhibits immunity during aging. Nature Immunology [Internet]. 2017;18(3):354–63. Available from: http://dx.doi.org/10.1038/ni.3665

20. Plunkett FJ, Franzese O, Finney HM, Fletcher JM, Belaramani LL, Salmon M, et al. The loss of telomerase activity in highly differentiated CD8+CD28-CD27-T cells is associated with decreased Akt (Ser473) phosphorylation. Journal of immunology (Baltimore, Md : 1950). 2007;178(12):7710–9.

21. Henson SM, Lanna A, Riddel NE, Franzese O, Macaulay R, Griffiths SJ, et al. P38 signaling inhibits mTORC1-independent autophagy in senescent human CD8+ T cells. Journal of Clinical Investigation. 2014;124(9):4004–16.

22. Campisi J, D'Adda Di Fagagna F. Cellular senescence: When bad things happen to good cells. Vol. 8, Nature Reviews Molecular Cell Biology. 2007.

23. Tchkonia T, Zhu Y, van Deursen J, Campisi J, Kirkland JL. Cellular senescence and the senescent secretory phenotype: Therapeutic opportunities. Vol. 123, Journal of Clinical Investigation. 2013. p. 966–72.

24. Pereira BI, de Maeyer RPH, Covre LP, Nehar-Belaid D, Lanna A, Ward S, et al. Sestrins induce natural killer function in senescent-like CD8+ T cells. Nature Immunology. 2020 Jun 1;21(6):684–94.

25. Pereira BI, Akbar AN. Convergence of innate and adaptive immunity during human aging. Frontiers in Immunology. 2016;7(NOV):1–9.

26. Xu W, Larbi A. Markers of T cell senescence in humans. Vol. 18, International Journal of Molecular Sciences. MDPI AG; 2017.

27. Covre LP, Devine OP, Garcia de Moura R, Vukmanovic-Stejic M, Dietze R, Ribeiro-Rodrigues R, et al. Compartmentalized cytotoxic immune response leads to distinct pathogenic roles of natural killer and senescent CD8+ T cells in human cutaneous leishmaniasis. Immunology. 2020 Apr 1;159(4):429–40.

28. Covre LP, Martins RF, Devine OP, Chambers ES, Vukmanovic-Stejic M, Silva JA, et al. Circulating senescent T cells are linked to systemic inflammation and lesion size during human cutaneous leishmaniasis. Frontiers in Immunology. 2019;10(JAN):1–12.

29. Amorim CF, Novais FO, Nguyen BT, Misic AM, Carvalho LP, Carvalho EM, et al. Variable gene expression and parasite load predict treatment outcome in cutaneous leishmaniasis [Internet]. Vol. 11, Sci. Transl. Med. 2019. Available from: http://stm.sciencemag.org/

30. R Core Team. R: A Language and Environment for Statistical Computing [Internet]. R Foundation for Statistical Computing. Vienna, Austria; 2020. Available from: https://www.r-project.org/

31. RStudio Team. Integrated Development for R. [Internet]. RStudio, PBC, Boston, MA. Boston, MA; 2020 [cited 2018 Jun 11]. Available from: https://www.rstudio.com/

32. Love MI, Huber W, Anders S. Moderated estimation of fold change and dispersion for RNA-seq data with DESeq2. Genome biology [Internet]. 2014;15(12):550. Available from: http://www.ncbi.nlm.nih.gov/pubmed/25516281

33. Avelar RA, Ortega JG, Tacutu R, Tyler EJ, Bennett D, Binetti P, et al. A multidimensional systems biology analysis of cellular senescence in aging and disease. Genome Biology. 2020;21(1).

34. Tacutu R, Thornton D, Johnson E, Budovsky A, Barardo Di, Craig T, et al. Human Ageing Genomic Resources: New and updated databases. Nucleic Acids Research. 2018;46(D1).

35. von Mering C, Jensen LJ, Snel B, Hooper SD, Krupp M, Foglierini M, et al. STRING: Known and predicted protein-protein associations, integrated and transferred across organisms. Nucleic Acids Research. 2005;33(DATABASE ISS.).

36. Frishberg A, Brodt A, Steuerman Y, Gat-Viks I. ImmQuant: a user-friendly tool for inferring immune cell-type composition from gene-expression data. Bioinformatics [Internet]. 2016 Dec 15;32(24):3842–3. Available from: https://academic.oup.com/bioinformatics/article-lookup/doi/10.1093/bioinformatics/btw535

37. Novais FO, Carvalho LP, Passos S, Roos DS, Carvalho EM, Scott P, et al. Genomic Profiling of Human Leishmania braziliensis Lesions Identifies Transcriptional Modules Associated with Cutaneous Immunopathology. Journal of Investigative Dermatology. 2015 Jan 1;135(1):94–101.

38. Birch J, Gil J. Senescence and the SASP: Many therapeutic avenues. Genes and Development. 2020;34(23–24).

39. Novais FO, Carvalho AM, Clark ML, Carvalho LP, Beiting DP, Brodsky IE, et al. CD8+T cell cytotoxicity mediates pathology in the skin by inflammasome activation and IL-1β production. PLoS Pathogens. 2017 Feb 1;13(2).

40. Velarde MC, Demaria M, Campisi J. Senescent cells and their secretory phenotype as targets for cancer therapy. Interdisciplinary Topics in Gerontology. 2013;38.

41. Henson SM, Akbar AN. KLRG1-more than a marker for T cell senescence. Age. 2009;31(4):285–91.

42. Zdanov S, Toussaint O, Debacq-Chainiaux F. p53 and ATF-2 partly mediate the overexpression of COX-2 in H2 O2-induced premature senescence of human fibroblasts. Biogerontology. 2009;10(3).

43. Moura RG de, Covre LP, Fantecelle CH, Alejandro V, Gajardo T, Cunha CB, et al. PD-1 Blockade Modulates Functional Activities of Exhausted-Like T Cell in Patients With Cutaneous Leishmaniasis. 2021;12(March):1–12.

44. Diaz NL, Zerpa O, Ponce L v., Convit J, Rondon AJ, Tapia FJ. Intermediate or chronic cutaneous leishmaniasis: Leukocyte immunophenotypes and cytokine characterisation of the lesion. Experimental Dermatology. 2002;11(1):34–41.

45. Campisi J, Kapahi P, Lithgow GJ, Melov S, Newman JC, Verdin E. From discoveries in ageing research to therapeutics for healthy ageing. Vol. 571, Nature. 2019.

46. Covre LP, Devine OP, Garcia de Moura R, Vukmanovic-Stejic M, Dietze R, Ribeiro-Rodrigues R, et al. Compartmentalized cytotoxic immune response leads to distinct pathogenic roles of natural killer and senescent CD8+ T cells in human cutaneous leishmaniasis. Immunology. 2020;159(4):429–40.

47. Childs BG, Durik M, Baker DJ, van Deursen JM. Cellular senescence in aging and age-related disease: From mechanisms to therapy. Vol. 21, Nature Medicine. 2015.

48. Schurich A, Henson SM. The many unknowns concerning the bioenergetics of exhaustion and senescence during chronic viral infection. Frontiers in Immunology. 2014;5(SEP):1–6.

49. Lanna A, Henson SM, Akbar A. THE REGULATION OF T CELL SENESCENCE AND METABOLISM BY P38 MAPKINASE SIGNALING. Innovation in Aging. 2017;1(suppl_1).

50. Macaulay R, Akbar AN, Henson SM. The role of the T cell in age-related inflammation. Age. 2013;35(3):563–72.

51. Mogilenko DA, Shpynov O, Andhey PS, Arthur L, Swain A, Esaulova E, et al. Comprehensive Profiling of an Aging Immune System Reveals Clonal GZMK+ CD8+ T Cells as Conserved Hallmark of Inflammaging. Immunity. 2021 Jan 12;54(1):99-115.e12.

52. Franceschi C, Capri M, Monti D, Giunta S, Olivieri F, Sevini F, et al. Inflammaging and anti-inflammaging: A systemic perspective on aging and longevity emerged from studies in humans. Mechanisms of Ageing and Development. 2007;128(1):92–105.

53. Carvalho AM, Novais FO, Paixão CS, de Oliveira CI, Machado PRL, Carvalho LP, et al. Glyburide, a NLRP3 Inhibitor, Decreases Inflammatory Response and Is a Candidate to Reduce Pathology in Leishmania braziliensis Infection. Journal of Investigative Dermatology. 2019;140(1):1-3.e2.

54. Bacellar O, Lessa H, Schriefer A, Machado P, de Jesus AR, Dutra WO, et al. Up-regulation of Th1-type responses in mucosal leishmaniasis patients. Infection and Immunity. 2002 Dec;70(12):6734–40.

55. Franceschi C, Campisi J. Chronic inflammation (Inflammaging) and its potential contribution to age-associated diseases. Journals of Gerontology - Series A Biological Sciences and Medical Sciences. 2014;69(October):S4–9.

56. Pinti M, Appay V, Campisi J, Frasca D, Fülöp T, Sauce D, et al. Aging of the immune system: Focus on inflammation and vaccination. Vol. 46, European Journal of Immunology. Wiley-VCH Verlag; 2016. p. 2286–301.

57. Groh V, Rhinehart R, Randolph-Habecker J, Topp MS, Riddell SR, Spies T. Costimulation of CD8αβ T cell by NKG2D via engagement by MIC induced on virus-infected cells. Nature Immunology. 2001;2(3).

58. Gasser S, Orsulic S, Brown EJ, Raulet DH. The DNA damage pathway regulates innate immune system ligands of the NKG2D receptor. Nature. 2005;436(7054).

59. Crosby EJ, Goldschmidt MH, Wherry EJ, Scott P. Engagement of NKG2D on Bystander Memory CD8 T Cells Promotes Increased Immunopathology following Leishmania major Infection. PLoS Pathogens. 2014;10(2).

60. Crosby EJ, Clark M, Novais FO, Wherry EJ, Scott P. Lymphocytic Choriomeningitis Virus Expands a Population of NKG2D + CD8 + T Cells That Exacerbates Disease in Mice Coinfected with Leishmania major. The Journal of Immunology. 2015 Oct 1;195(7):3301–10.

61.   Novais FO, Scott P. CD8+ T cells in cutaneous leishmaniasis: the good, the bad, and the ugly. Vol. 37, Seminars in Immunopathology. Springer Verlag; 2015. p. 251–9.

Legends of figures, supplementary figures and supplementary tables

Figure 1. Differentially expressed genes demonstrate senescence profile. A) Gene ontology overrepresentation analysis of all DEGs. The selected categories were all significantly enriched with p adjusted value < 0.05. Size of the circles was used to distinguish the number of genes in each category. B) Immune cell deconvolution using ImmQuant software. Values represent relative score based on mean of all samples in each cell type. C) Dotplots and boxplots of selected cell populations from deconvolution analysis where groups are compared by Wilcoxon rank-sum test. HC, Healthy controls; LCL, Localized Cutaneous Leishmaniasis patients.

Figure 2. Senescence-associated genes are conspicuous in CL lesions. A) Violin plot of selected key senescence-associated genes. Gene expression is represented as log2 normalized and variance stabilized (vst) values, with corresponding adjusted p-values as calculated by DESeq2, where healthy controls (HC, light blue) and lesions from LCL patients (LCL, red) are compared. B) Spearman correlations between the selected senescence genes from A and the number of parasites detected by qPCR in lesions of patients. C) Correlation between expression of selected senescence genes from A and predicted cell population scores calculated by ImmQuant. HC, healthy controls. LCL, Localized Cutaneous Leishmaniasis.

Figure 3. Senescence-associated secretory phenotype- SASP, inflammatory cytokine and chemokine genes show are overrepresented in CL lesions and are correlated senescent cells. A) MA plot highlighting genes that were differentially expressed in the referred categories. Light grey represents non-significant genes, medium-grey represents underrepresented genes and dark-grey represents overrepresented genes. Indicated are the top 12 overrepresented genes from B. B) Violin plots showing the marked increase of the top 12 overrepresented SASP genes. Gene expression is represented as normalized and variance stabilized (vst) values, with corresponding adjusted p-values

as calculated by DESeq2, where healthy controls (HC, light blue) and lesions from LCL patients (LCL, red) are compared. C) Two heatmaps are shown. The heatmap on the left shows differentially expressed from the corresponding categories, comparing skin biopsies from healthy controls (HC, light blue) and lesions from LCL patients (LCL, red). Gene expression is represented in relative normalized and variance stabilized (vst) expression values (centred in row means), ranging from cyan (underrepresented) to yellow (overrepresented). Each row corresponds to a single gene and each column to a subject. The heatmap on the right represents the spearman correlation (ranging from dark blue to dark red) of expression of the same genes to predicted cell population scores calculated by ImmQuant. NS, non-significant. HC, healthy controls. LCL, Localized Cutaneous Leishmaniasis.

Figure 4. Senescent cells accumulate in CL lesions and correlate with the disease severity. Immunofluorescence staining and cumulative data of the expression of (A, C) KLRG1 and (B, E) ATF in the lesions of patients with CL (LCL) and in healthy skin (HC). (D, F) Fold changes of KLRG1 (7.18-fold increase) gene and the ATF (5.67-fold increase) gene with highest upregulation in CL lesions. (G, H) Pearson's correlation test between the expression of senescence markers and lesion size (mm^2). The graphs show the mean ± SD. Scale bar: 100 µm.

Supplementary figure 1. Gene expression of CL lesions are distinct from healthy skin controls. A) Heatmap of all differentially expressed genes (DEGs) in the dataset, comparing skin biopsies from healthy controls (HC, light blue) and lesions from LCL patients (LCL, red). Gene expression is represented in relative normalized and variance stabilized (vst) expression values (centred in row means), ranging from cyan (underrepresented) to yellow (overrepresented). Each row corresponds to a single gene and each column to a subject. B) Principal component analysis comparing healthy controls (light blue, HC) and lesion skin (red, LCL). C) Volcano plot showing all differentially expressed genes according to DESeq2 analysis. Horizontal dashed line represents p =

0.05 threshold, where grey dots correspond to non-significant genes, medium blue dots to underrepresented genes and medium red to overrepresented genes.

Supplementary figure 2. Replicative senescence genes are overrepresented in CL lesional skin. A) Heatmap of all differentially expressed genes, with foldchange cut-offs of 2 and -2, from the CellAge database, with the addition of other immunosenescence genes, comparing skin biopsies from healthy controls (HC, light blue) and lesions from LCL patients (LCL, red). Gene expression is represented in relative normalized and variance stabilized (vst) expression values (centred in row means), ranging from cyan (underrepresented) to yellow (overrepresented). Each row corresponds to a single gene and each column to a subject. B) Network analysis showing interactions between overrepresented and underrepresented differentially expressed genes (foldchange cut-offs of >2 and <-2) from senescence database analysis.

Supplementary figure 3. Correlation between selected senescence genes and patient data. Plots show the Spearman correlations between the selected senescence genes (Fig. 2A) and A) age and B) healing time (days to cure) of patients in the RNASeq dataset.

Supplementary figure 4. Violin plots of SASP differentially expressed genes. Gene expression is represented as log2 normalized and variance stabilized (vst) values, with corresponding adjusted p-values as calculated by DESeq2, where healthy controls (HC, light blue) and lesions from LCL patients (LCL, red) are compared.

Supplementary figure 5. Violin plot of selected cytokines, chemokines and receptor differentially expressed genes. A) Violin plots showing the selected differentially expressed Cytokines and Cytokine receptors genes. B) Violin plots showing the selected differentially expressed Chemokines and Chemokine receptors genes. Gene expression is represented as log2 normalized

and variance stabilized (vst) values, with corresponding adjusted p-values as calculated by DESeq2, where healthy controls (HC, light blue) and lesions from LCL patients (LCL, red) are compared.

Supplementary Table 1. Table showing the results from DESeq2 analysis of all differentially expressed genes in the dataset. Differentially expressed genes were defined as genes with adjusted p-value < 0.05.

Supplementary Table 2. Table showing the results from CellAge database and immunosenescence genes analysis of differential expression. Differentially expressed genes were defined as genes with adjusted p-value < 0.05.

Supplementary Table 3. Table showing protein-protein interactions from the STRING database for overrepresented and underrepresented senescence genes. Interactions between overrepresented and underrepresented genes are stored in the first and second sheets, respectively. A STRING score of 700 was used as threshold for interactions.

Supplementary Table 4. Table showing the genes selected for the corresponding categories (Cytokines and cytokine receptors, chemokines and chemokine receptors and SASP) and the results of the differential expression analysis for these genes. Differentially expressed genes were defined as genes with adjusted p-value < 0.05.
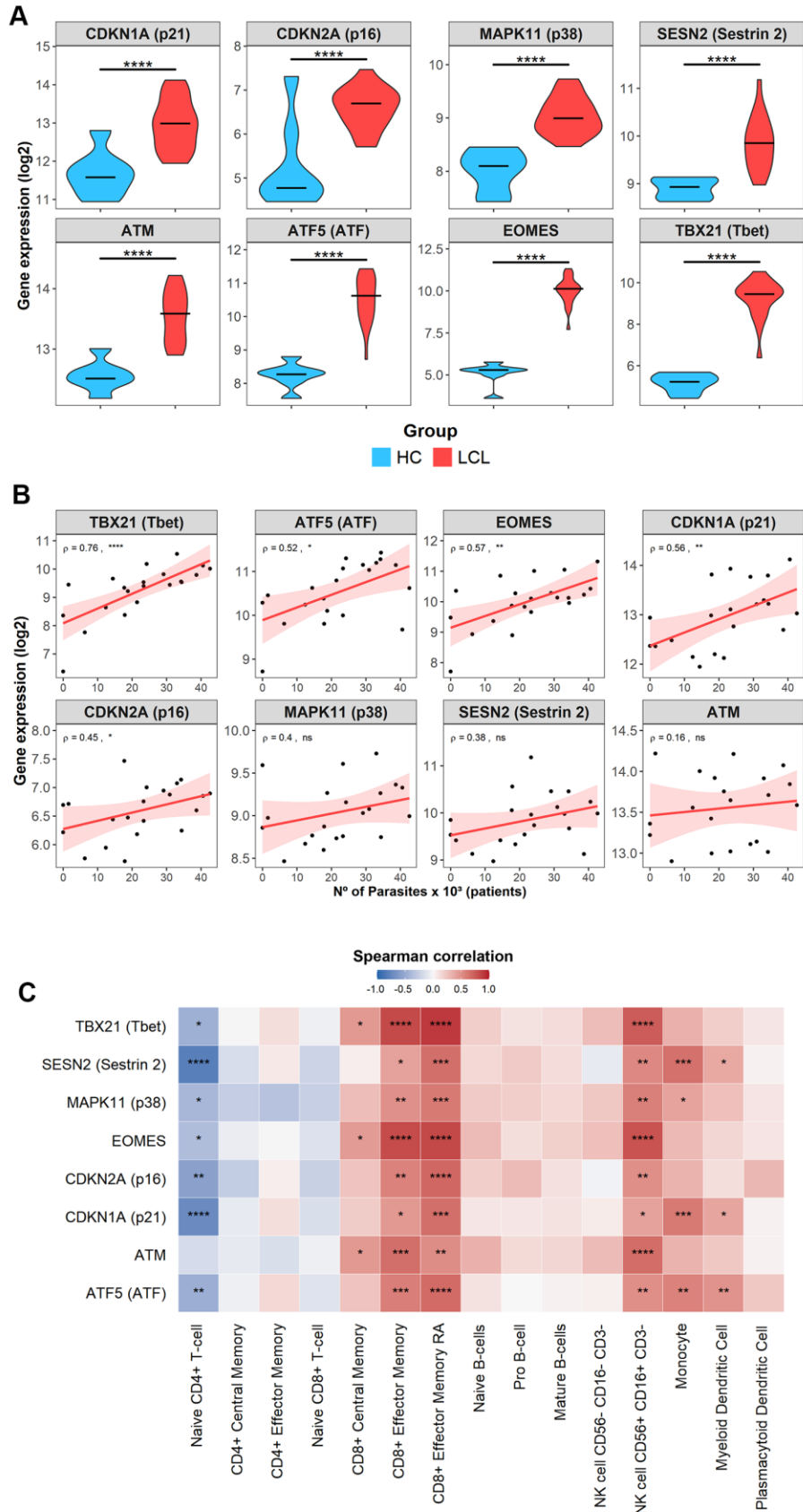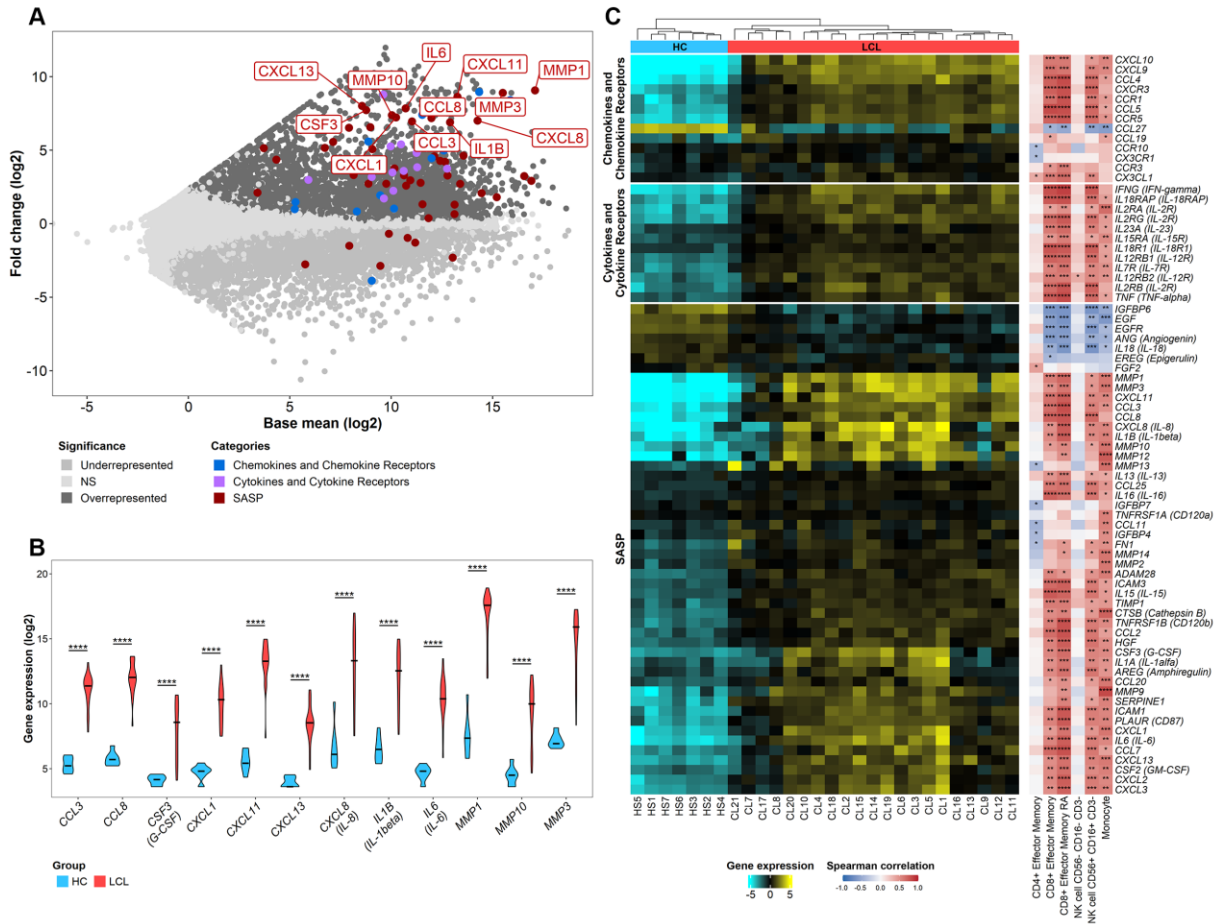
Figure 1
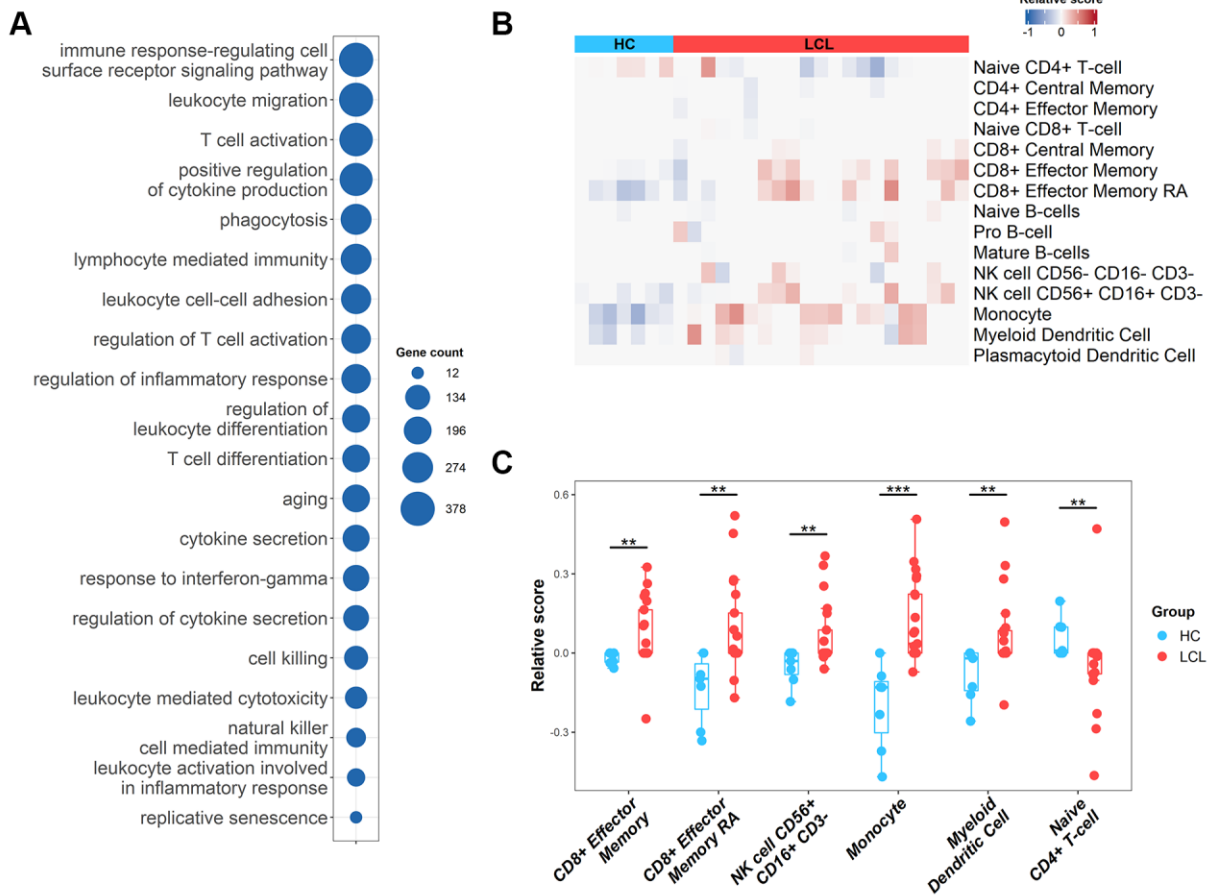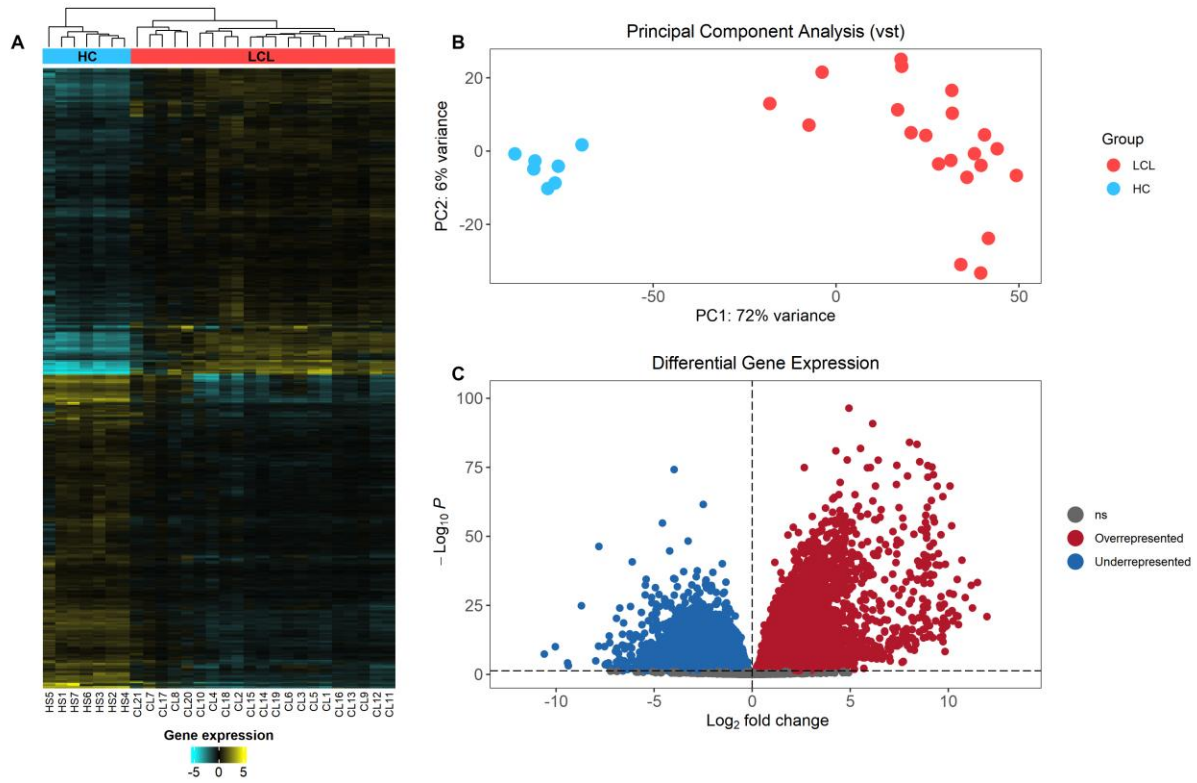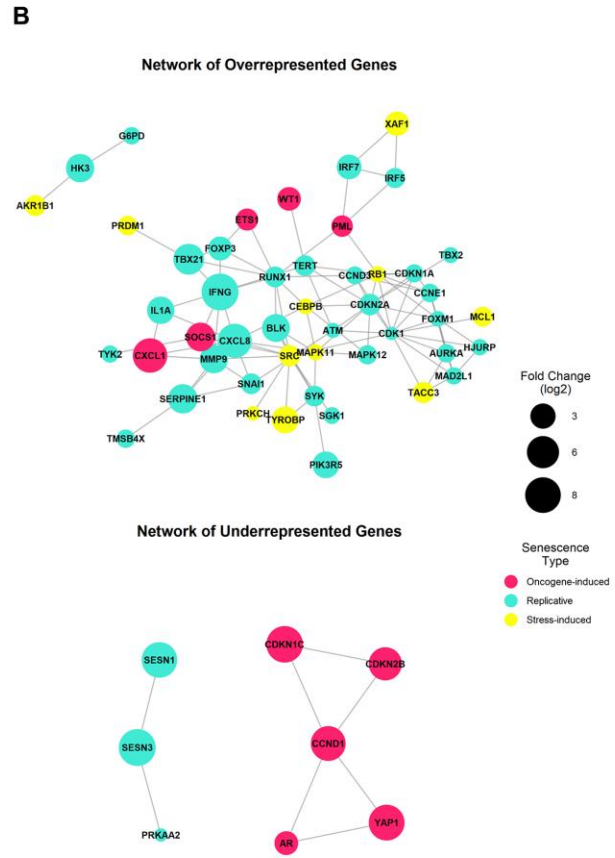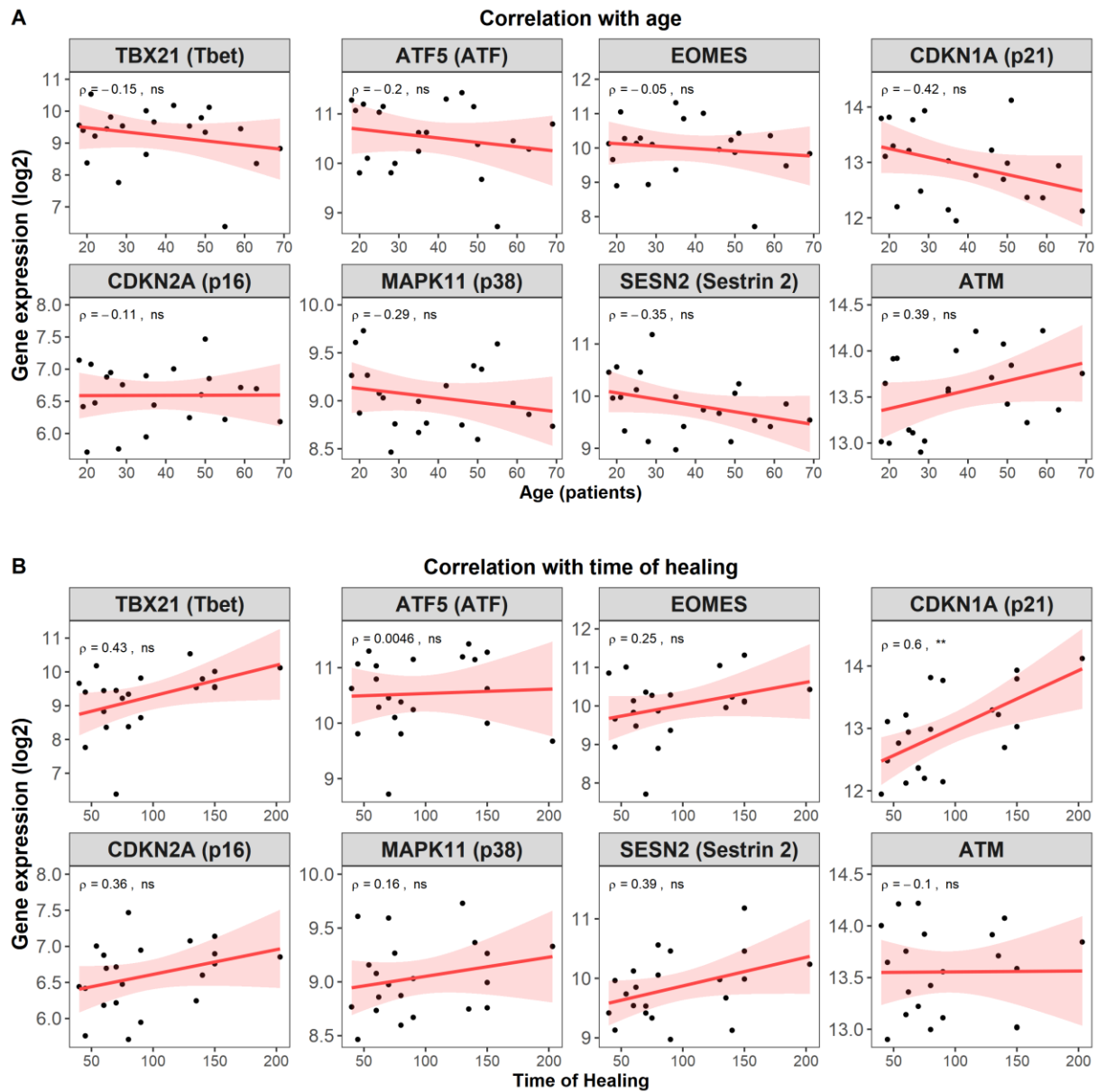
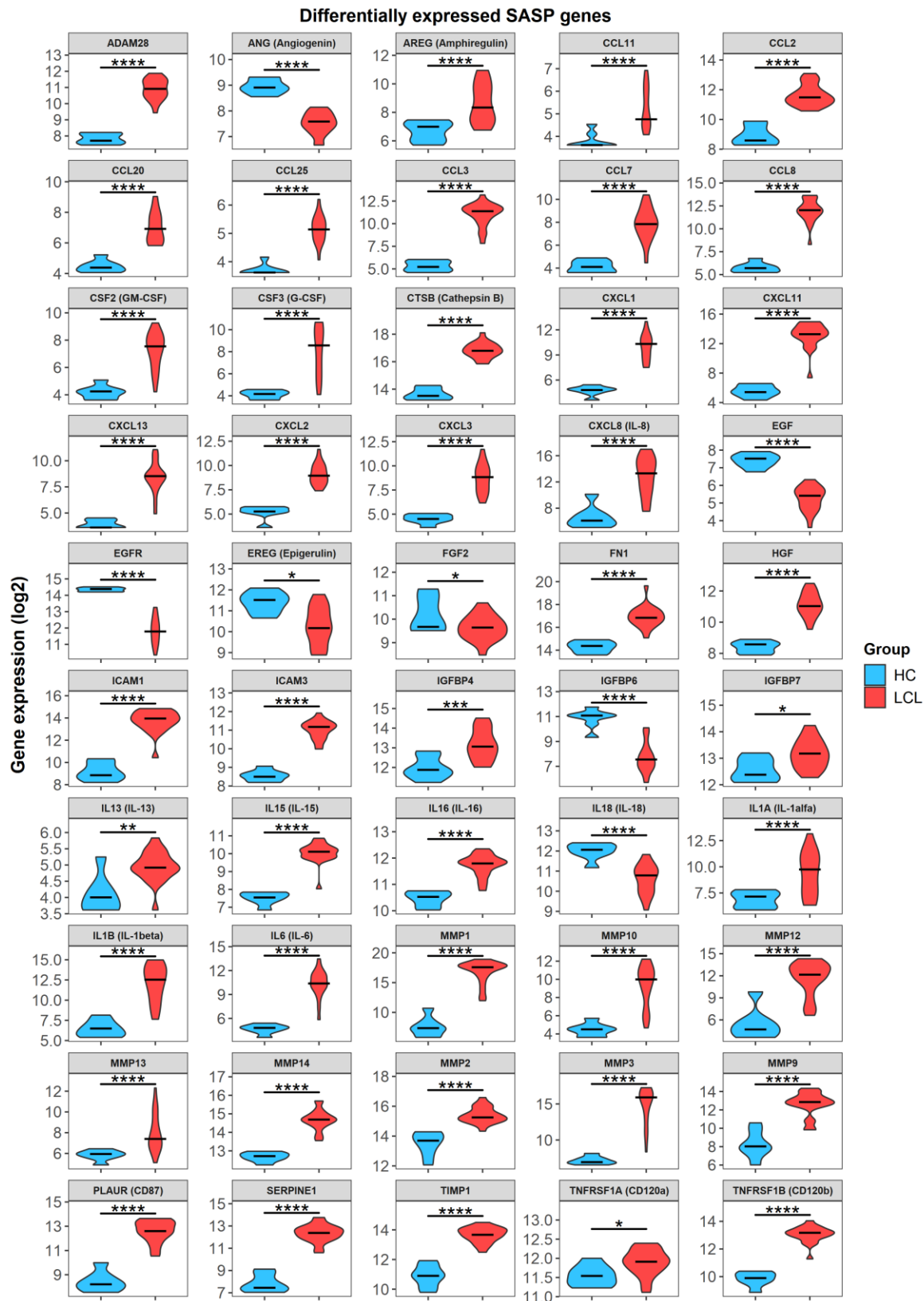**Figure 2**

Figure 3

Figure 4
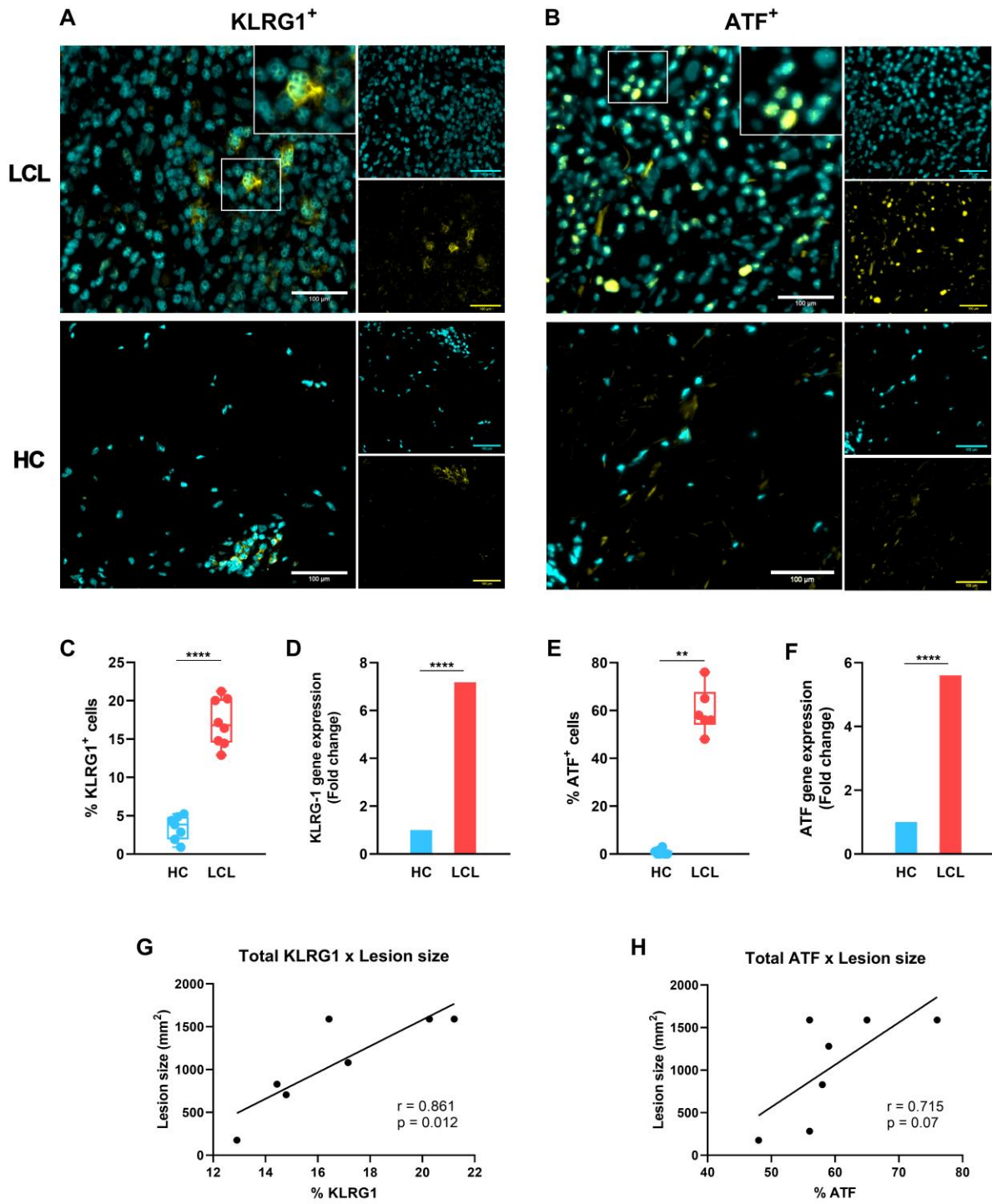
Supplementary figure 1

Supplementary figure 2
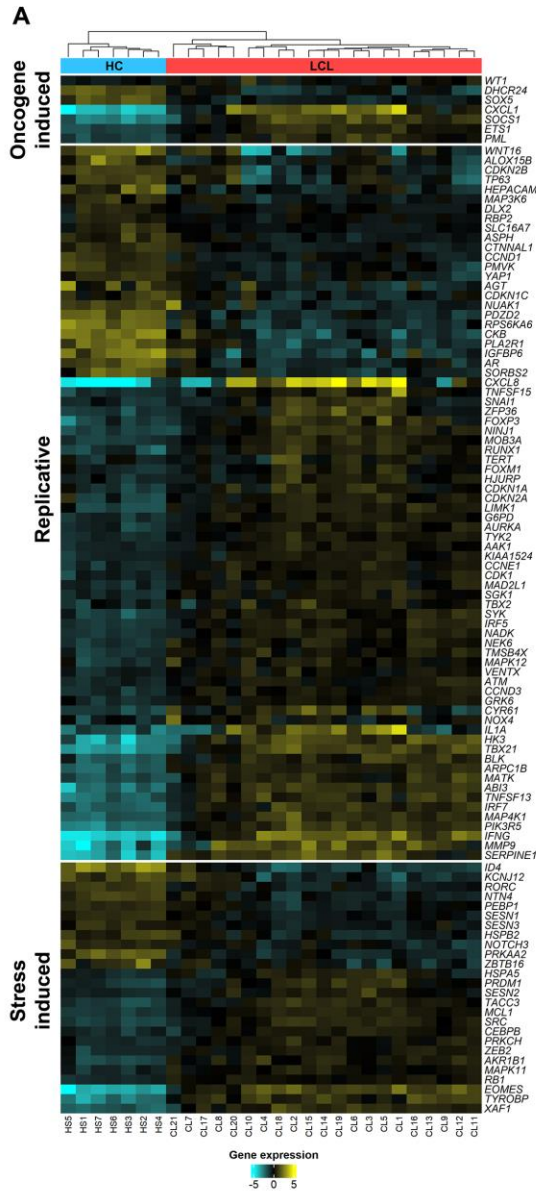
Supplementary figure 3

Supplementary figure 4

Differentially expressed SASP genes

Supplementary figure 5

A   Differentially expressed Cytokine and Receptors genes

B   Differentialy expressed Chemokine and Receptors genes